Desalination and Water Treatment
www.deswater.com

1944-3994/1944-3986 © 2011 Desalination Publications. All rights reserved
doi: 10/5004/dwt.2012.2822

42 (2012) 202–209
April

Lead(II) biosorption of an Antarctic sea-ice bacterial exopolysaccharide

Yuhong Ma[a], Boling Shen[a], Ruilian Sun[b], Weizhi Zhou[a,c,*], Yuzhong Zhang[c]

[a]*School of Environmental Science and Engineering, Shandong University, Jinan 250100, PR China*
[b]*Environment Research Institute, Shandong University, Jinan 250100, PR China*
[c]*State Key Laboratory of Microbial Technology, Shandong University, Jinan 250100, PR China*
Tel. +86 531 88361383; Fax: +86 531 88361383; email: wzzhou@sdu.edu.cn

Received 2 June 2011; Accepted 20 November 2011

ABSTRACT

Biosorption behavior and mechanism of an exopolysaccharide (EPS) secreted by a psychrotolerant bacterium *Pseudoalteromonas* sp. Bsi20310 isolated from Antarctic sea-ice, for lead(II) from synthetic wastewater were studied in this paper. Effects of salinity, pH and dosage of Bsi20310 EPS on biosorption characteristics for lead(II) were evaluated by batch biosorption tests. The results indicated that Bsi20310 EPS presented better biosorption performance for lead(II) in salt water than in salt-free water. The equilibrium biosorption isotherms fitted well to both Langmuir and Freundlich isotherm models. Theoretical maximum biosorption capacity of 191.90 mg g^{-1} calculated according to Langmuir equation indicated that Bsi20310 EPS had a high biosorption capacity for lead(II). The kinetics of lead(II) biosorption onto Bsi20310 EPS could be better described by pseudo-second-order model than pseudo-first-order both in salt-free water and in salt water. External surface biosorption was the major biosorption mechanism while intraparticle diffusion was not the unitary rate-limiting step for the whole biosorption. Fourier transform infrared spectroscopy (FT-IR) analysis indicated that the functional groups such as –OH, C=O and C–O–C on Bsi20310 EPS may play important roles as biosorption sites in lead(II) biosorption.

Keywords: Lead(II) biosorption; Isotherms; Kinetics; Antarctic sea-ice bacterium; Salt water; Exopolysaccharide

1. Introduction

Heavy metals are increasingly introduced into water-bodies from industries of mining, electroplating, alloy preparation, pulp-paper, fertilizer and so forth [1,2]. Pollution of heavy metals has become an imperative concern on their accumulation in food chain and serious health hazards caused to living organisms [3]. Presence of lead in drinking water above the mandatory limit of 0.05 mg l^{-1} may cause adverse health effects to human beings such as anemia, encephalopathy, hepatitis and nephritic syndrome [4,5]. Many methods have been brought forward to remove heavy metals from wastewater and among which biosorption is a promising technology characterized by high biosorption capacity and selectivity, low cost and environmental safety [6,7]. Some reports indicated that the microbial exopolysaccharides (EPS) play important roles in metal biosorption, for instances of the EPSs secreted by fungus *Pestalotiopsis* sp. KCTC 8637P [8], cyanobacterium *Lyngbya putealis* HH-15 [9], bacterium *Paenibacillus polymyxa* CHL 0102 [10] and deep-sea mesophilic bacterium

---

*Corresponding author.

2011 Qingdao International Desalination Conference Symposium on Desalination and Water Treatment Global Platform for Water Solutions, June 20–23, 2011 Qingdao, China

Wangia profunda SM-A87 [11,12], etc. Previous work mainly focused on salt-free wastewater treatment, and only a few studies have been considered for salt water [12,13]. However, high quantities of salts accompanied with heavy metal in some industrial effluents as tanneries makes the removal of heavy metals more difficult and causes severely adverse effects on the sequential microbial activity [14]. Coexisted salts impaired the biosorption of heavy metals diversely by leading to high ionic strength and/or influencing the binding affinity between heavy metals and biosorbents [12,15]. It was found that increasing the salinity up to 20% (W/V) led to a significant decrease of biosorption capacity of chromium(VI) [16]. Although there are abundant reports on sorbents for heavy metal removal from wastewater, very few are for from salt water. It has significance to find biosorbents for heavy metal removal from salt water.

Antarctic microbes often secret a large amount of EPS to protect themselves against the harsh conditions such as low temperature and high salinity. During the dehydration-saturation turns caused by high seawater salinities and ice melting, the ice-trapped bacteria may experience salinities three times that of sea water to hyposaline conditions [17]. Though the mechanism was not so clear, it can reasonably be speculated that Antarctic EPSs played a major role in protecting organisms within ice floes from ice-crystal damage, buffer against pH and salinity changes, and ameliorate other chemical stresses like heavy metals [17]. It has been demonstrated that EPSs produced by sea-ice isolates possess a molecular weight 5–50 times larger than the average of the other isolated marine EPSs [18]. Due to their attractive structure and physicochemical properties, EPSs produced by sea-ice isolates may act as promising biosorbents for heavy metals removal in salt water treatment.

Bsi20310 EPS used as a biosorbent in this study was secreted by a psychrotolerant bacterium *Pseudoalteromonas* sp. Bsi20310, isolated from Antarctic sea-ice, which could grow in a wide range of salinity from 0% to 10%. The present work focused on the biosorption characteristics of Bsi20310 EPS for lead(II) from salt-free wastewater and salt water. Effect of salinity on bacteria growth, EPS yield and biosorption capacity was investigated. The biosorption isotherms, kinetics and potential functional groups were also investigated to explore the possible mechanism of lead(II) biosorption onto Bsi20310 EPS.

2. Materials and methods

2.1. Cultivation of *Pseudoalteromonas sp. Bsi20310* and preparation of Bsi20310 EPS

Pseudoalteromonas sp. Bsi20310 was isolated from Antarctic sea-ice, which could grow in a wide range of salinity from 0 to 10%. In this study, *Pseudoalteromonas* sp. Bsi20310 was first cultivated in the laboratory to secret EPS. Bsi20310 EPS was then separated and purified following the procedure reported elsewhere [19]. To obtain the optimal salinity for the growth of Bsi20310, the optical density of bacterial suspension was detected by spectrophotometer (UV-752, Shanghai) at 600 nm after fermentation in 2216E culture for 3 h at different salinities. The effect of salinity on Bsi20310 EPS yield was also tested.

2.2. Examination of zeta-potential of Bsi20310 EPS

Zeta-potential of Bsi20310 EPS (50 mg l^{-1}) was examined with 3000HSA ZetaSizer (Malvern, UK), at initial pH range of 4–8 and salinity range of 2.0–4.8%, respectively.

2.3. Preparation of synthetic lead(II) wastewater

Two types of lead(II) wastewater were prepared by dissolving $Pb(NO_3)_2$ in deionized water and salt solution, respectively. The salt solution was simulated by dissolving 33.3 g sea salt (Qingdao Haida, China) in 1 l deionized water. The solution pH was then adjusted to 5.5 by adding 0.5 mol l^{-1} HNO_3 or NaOH solutions.

2.4. Biosorption tests

For batch biosorption tests, known amount of Bsi20310 EPS was added to 50 ml lead(II) solution of 10 mg l^{-1} in a 250 ml conical flask and shaken (200 rpm) at 20°C for 2h. The solution was then filtered through ultra filtration membrane (10 kDa) and the concentration of residual lead(II) in the filtrate was measured using an Atomic Absorption Spectrophotometer (TAS-990, Purkinje General). Deuterium lamp background correction was used to reduce the disturbance of sea salt on lead(II) measurement. Blank samples were also measured by replacing Bsi20310 EPS solution with deionized water. All tests were carried out in triplicate and the mean values were reported.

The metal uptake (Q, mg g^{-1}) can be determined from Eq. (1):

$$Q = V\left(C_o - C_e\right)/W \qquad (1)$$

where C_o and C_e are the concentrations of initial and equilibrium lead(II) in the solution (mg l^{-1}), respectively; V is the solution volume (l); W is the mass of Bsi20310 EPS added (g).

2.5. Biosorption isotherms

During the experiments for biosorption isotherms, precipitation of Pb(II) hydroxide occurred at Pb(II) concentration upper than 100 mg l^{-1} in salt water, which was unfavorable for biosorption isotherms analysis for salt water. Therefore, biosorption isotherms for only salt-free water were analyzed while data for salt water were not enough for isotherms analysis. Biosorption isotherms for salt-free water were analyzed by a batch equilibrium assays. 1 ml of 2 g l^{-1} Bsi20310 EPS solution was added in 250 ml conical flask containing 50 ml lead(II) with the concentration range of 10–500 mg l^{-1}. The pH of the mixture was maintained at 5.5. The samples were shaken (200 rpm) at 20°C for 12 h to make sure the biosorption had reached equilibrium, then filtered and analyzed following the same processes described in Section 2.4.

2.6. Biosorption kinetics

For kinetic measurement, 1 ml of 2 g l^{-1} Bsi20310 EPS solution and 50 ml of 10 mg l^{-1} lead(II) solution were mixed and shaken at different intervals, then the procedures described in Section 2.4 were conducted.

2.7. FT-IR analysis

The dried Bsi20310 EPS samples before and after biosorption were pressed into KBr pellets at sample: KBr ratio of 1:100, then tested by an FT-IR spectrometer (VERTEX-70, BRUKER, FT-IR). The spectra were recorded in transmittance mode in the wave number range of 4000–400 cm^{-1}, at a resolution of 4 cm^{-1}.

3. Results and discussion

3.1. Effect of salinity on biosorption

The concomitant cations and anions often affect the efficiency of adsorption for the target heavy metals [12,15]. The effects of salinity on the lead biosorption by Bsi20310 EPS and the zeta-potential of EPS are shown in Fig. 1(a). The biosorption increased with the increase of salinity until 3.4% (around the salinity of actual seawater), and then reduced at greater salinities. On the contrary, the zeta-potential of Bsi20310 EPS steadily increased with the increase of salinity, indicating that the negative charge of Bsi20310 EPS steadily decreased, which was unfavorable for electrostatic biosorption. The results indicated that electrostatic biosorption was not the only mechanism of lead biosorption by Bsi20310 EPS in salt water. Effects of salinity on bacteria growth and Bsi20310 EPS yield shown in Fig. 1(b) and (c), respectively, were also in good agreement with the effect of salinity on biosorption.

Generally, salinity is an important factor affecting the microbial morphology, microbial growth, their cell composition and extracellular polymeric substance yield [20]. For example, Mishra and Jha [21] reported that extracellular polymeric substances produced by *Dunaliella salina* strain, increased concomitantly with salt concentration. Vyrides and Stuckey [22] reported that a higher production of EPS was obtained from biomass exposed to higher salt concentrations, and its composition was found to change under different saline conditions. Antarctic microbes often secret a large amount of poly substances, especially polysaccharide to protect themselves against the harsh Antarctica conditions, like low temperature and high salinity. Generally, Antarctica

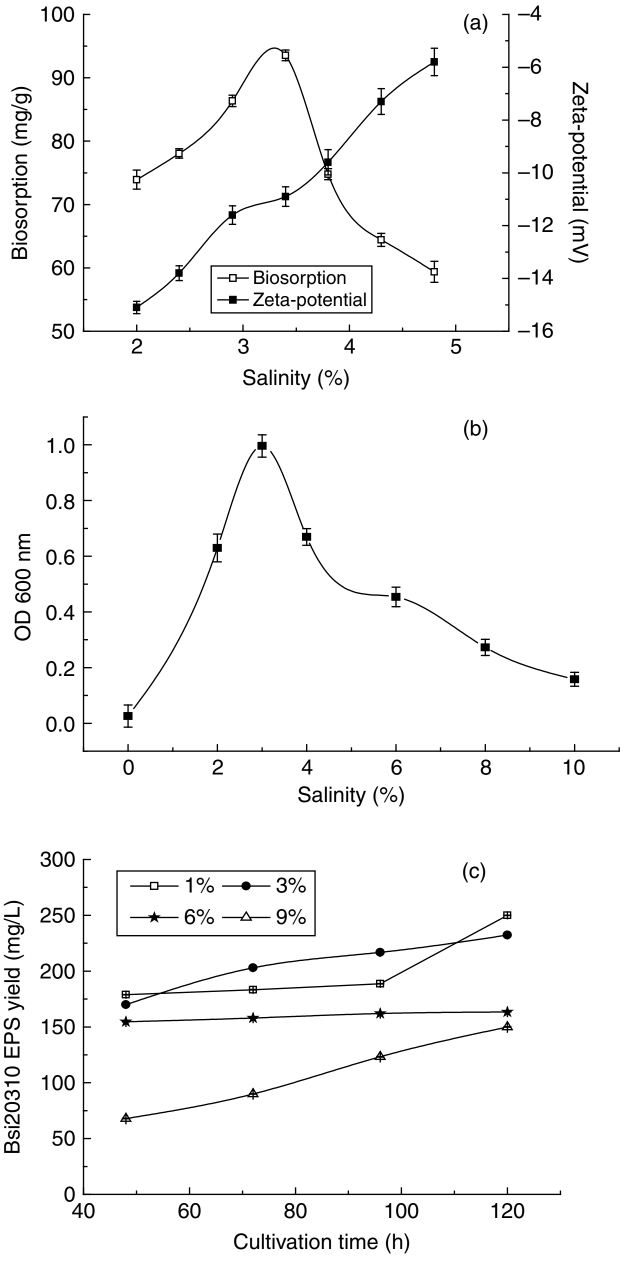

Fig. 1. Effect of salinity on (a) biosorption and zeta-potential; (b) bacteria growth; (c) Bsi20310 EPS yield.

sea-ice bacteria must experience great salinity gradients. When dehydration occurs, caused by the high brine salinities, the ice-trapped bacteria may experience salinities three times that of seawater. Conversely, when the ice melts, the released organisms would be suddenly exposed to hyposaline conditions close to salt-free water values [17]. The excellent regulation capacity of Bsi20310 EPS to salinity variations may be one of the reasons for the strong biosorption ability of Bsi20310 EPS.

In the present research, the salinity around 3% was the favorite salinity for bacteria growth, Bsi20310 EPS production and lead biosorption, which indicated that Bsi20310 EPS may be considered as a promising adsorbent for lead in seawater environment.

3.2. *Effect of initial pH on biosorption*

Solution pH is an important parameter in the biosorption process, because it affects both the metal speciation and Bsi20310 EPS state (especially its surface charge), consequently affects their adsorbing reaction [3,23]. The effect of pH on biosorption capacity is shown in Fig. 2. In both systems, the biosorption capacity of Bsi20310 EPS for lead(II) increased with pH increasing. Except pH value range of 2.0–4.0, where the biosorption capacity were ineffectively low in two systems, the biosorption capacity of Bsi20310 EPS for lead(II) was obviously higher in salt water than in salt-free water at other pH values. The reaction of lead(II) with Bsi20310 EPS can be described by the following equilibrium [12]:

$$mM^{n+} + nH_mB \Leftrightarrow nmH^+ + M_mB_n \tag{2}$$

where M^{n+} represents the metal ions possessed *n* charges, B is the available biosorption sites on the EPS. It can be seen from Eq. (2) that the amount of formed M_mB_n was mainly affected by the concentration of H_3O^+ due to the competition between H_3O^+ and metal ions for biosorption sites. At lower pH, such sites on the EPS were not available due to the existence of large amounts of H_3O^+ in solution. With pH increasing, the deprotonation of acid functional groups were strengthened and these negatively charged groups on Bsi20310 EPS surface showed greater biosorption force for lead(II) [12]. This can also be supported by the zeta-potential change with solution pH as shown in Fig. 2. Zeta-potential of Bsi20310 EPS was minus and the negative charge of EPS increased with the increase of pH, indicating that Bsi20310 EPS should have a higher potential to adsorb positively charged lead(II) ions. At pH 4–5.5, the sharp ascent of biosorption capacity in salt-free water and salt water was corresponding to the sharp decline of the zeta-potential of Bsi20310 EPS.

3.3. *Effect of Bsi20310 EPS dosage on biosorption*

The effect of Bsi20310 EPS dosage on lead(II) biosorption is shown in Fig. 3. The biosorption of lead(II) by Bsi20310 EPS decreased from 118.10 to 22.24 mg g^{-1} in salt-free water and from 159.44 to 45.62 mg g^{-1} in salt water, respectively, by increasing the EPS dosage from 8 to 182 mg l^{-1} under equilibrium conditions. This also verified that the lead(II) biosorption on Bsi20310 EPS was more favorable in salt water than in salt-free water. The decrease in lead(II) biosorption capacity at increasing Bsi20310 EPS dosage could be attributed to the decreased ratio of metal to biosorbent. This decrease led to more biosorption sites of the adsorbent remaining unsaturated during the biosorption process. The low incommensurate utilization of the biosorption sites of the adsorbent made the lower adsorptive capacity. Similar tendencies were found in heavy metal biosorption process reported in references [24].

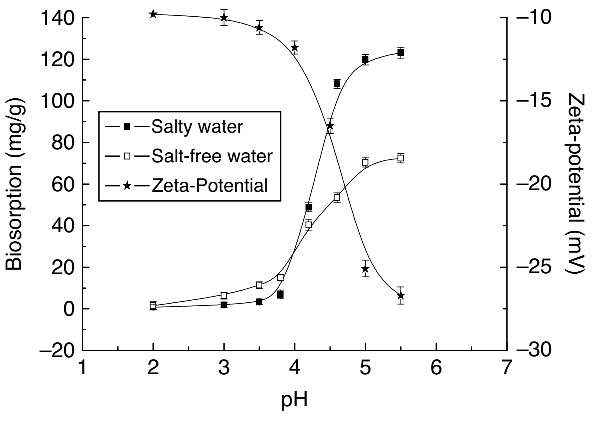

Fig. 2. Effect of initial pH on biosorption and zeta-potential of Bsi20310 EPS.

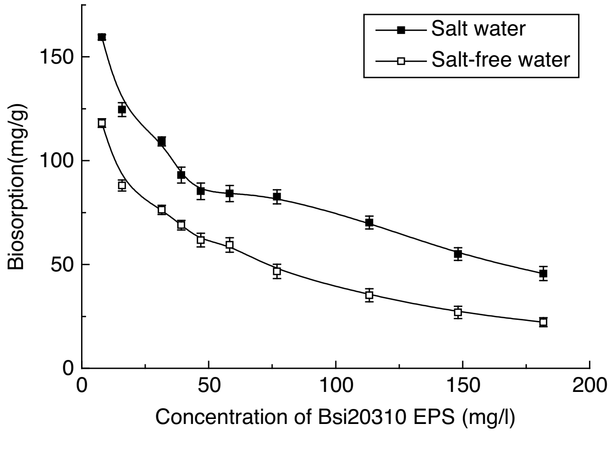

Fig. 3. Effect of Bsi20310 EPS dosage on biosorption.

3.4. Biosorption isotherms

The distribution of metal ions between aqueous solution and adsorbents at equilibrium of biosorption process can be generally described by several isotherms to evaluate the biosorption features of adsorbents (e.g., biosorption capacity or intensity). The most frequently employed isotherm equations are Langmuir and Freundlich models [25].

The Langmuir isotherm can be expressed as the linear equation:

$$1/Q_e = 1/Q_m + 1/(Q_m K_L C_e) \quad (3)$$

where C_e and Q_e are the concentrations of metal in solution at equilibrium (mg l^{-1}) and equilibrium biosorption capacity for metal (mg g^{-1}), respectively; K_L is the Langmuir equilibrium constant (l mg^{-1}), Q_m is the maximum biosorption capacity (mg g^{-1}). The values of Q_m and K_L for the biosorption of lead(II) onto Bsi20310 EPS can be derived from the linear plot of $1/Q_e$ versus $1/C_e$, respectively.

The Freundlich isotherm is linearized as follows:

$$\ln Q_e = \ln K_F + 1/n \ln C_e \quad (4)$$

where K_F indicates biosorption capacity and n is an empirical constant related to biosorption intensity of the adsorbent. For values in the range of $1 < n < 10$, biosorption is favorable [25].

Biosorption functioned on initial Pb(II) concentration is shown in Fig. 4. And all parameters correlating with the Langmuir and Freundlich equations and the corresponding correlation coefficients (R^2) are given in Table 1. It was shown that Bsi20310 EPS had higher biosorption capacity in salt water than in salt free water at low concentration of Pb(II). However the precipitation of Pb(II) hydroxide occurred at Pb(II) concentration upper than 100 mg l^{-1} in salty water as shown in Fig. 4. Precipitation of Pb(II) increased with increase of initial concentration of Pb(II) after salt addition. This made it unfavorable to test the biosorption isotherms. Therefore, biosorption isotherms for only salt-free water were analyzed while those for salty water were not reported.

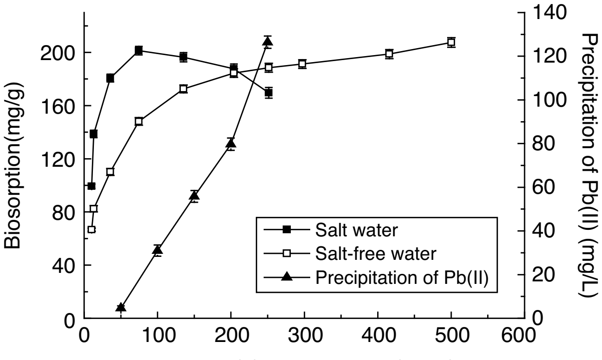

Fig. 4. Effect of initial Pb(II) concentration on biosorption.

Table 1
Isotherm parameters obtained from Langmuir and Freundlich models for lead(II) biosorption onto Bsi20310 EPS in salt-free water

Langmuir			Freundlich		
Q_m (mg g^{-1})	K_L (l mg^{-1})	R^2	K_F (g l^{-1})	n	R^2
191.90	0.054	0.972	38.53	3.48	0.978

According to the correlation coefficients, both Langmuir and Freundlich models can represent the biosorption isotherm of lead(II) onto Bsi20310 EPS. The maximum biosorption capacity Q_m calculated according to Langmuir isotherm was 191.90 mg l^{-1}. The value of Freundlich constant n was 3.48, indicating that the strength of metal biosorption by the biosorbent was quite intense. Bsi20310 EPS was an effective and favorable adsorbent for lead(II).

The biosorption capacities of various biosorbents towards Pb(II) as reported in literature have been presented in Table 2. A comparison between this work and other reported data showed that Bsi20310 EPS is a better biosorbent for Pb(II) compared to other biosorbents. [26,27]. Consideration of the better performance of Bsi20310 EPS at low concentration of Pb(II) in salt water than in salt free water, it could be safely concluded that the biomass of Bsi20310 EPS has a considerable potential for the removal of Pb(II) from an aqueous solution.

3.5. Biosorption kinetics

The most widely used kinetic models, namely pseudo-first-order and pseudo-second-order were applied to describing the biosorption rate of lead(II) onto Bsi20310 EPS. In addition, the intraparticle diffusion model was introduced to evaluate the role of diffusion in biosorption to understand the mechanism deeply [28].

The pseudo-first-order model of Lagergren is given as:

$$\log(Q_e - Q_t) = \log Q_e - k_1 t/2.303 \quad (5)$$

The pseudo-second-order model is as follows:

$$t/Q_t = 1/(k_2 Q_e^2) + t/Q_e \quad (6)$$

Table 2
Comparison of biosorption capacity of Bsi20310 EPS with different biosorbents

Biosorbent	Maximum biosorption capacity (mg g^{-1})	pH	Temperature (K)	Ref.
Bsi20310 EPS	191.90	5.5	293	This work
Acacia leucocephala bark powder	185.2	4.0	303	[2]
FCCL	75.82	5.0	333.2	[3]
PLAC	99.01	5.0	313	[5]
Calophyllum inophyllum	34.51	4.0	323	[6]
Moringa olifera bark	34.6	5.0	298	[7]
Exopolysaccharides	357	5.5	303	[11]
Waste beer yeast	5.71	5.0	293	[13]
CAMOL	209.54	5.0	313	[26]
Pecannut shell	211.7	5.5	293	[27]
PLAC	98.39	5.0	298	[30]

where k_1 (min^{-1}) and k_2 [g (mg min)$^{-1}$] are the rate constants of pseudo-first-order model and pseudo-second-order model, respectively. Q_e and Q_t (mg g^{-1}) are the amounts of metal adsorbed on Bsi20310 EPS at equilibrium and at time t, respectively.

The intraparticle diffusion equation can be expressed as:

$$Q_t = k_{pi}t^{0.5} + C_i \quad (7)$$

where k_{pi} [mg (g min$^{1/2}$)$^{-1}$] is the intraparticle diffusion rate constant of stage i, and C_i is the intercept of stage i.

Plots of linearized forms corresponding to pseudo-first-order and pseudo-second-order kinetic models are presented in Fig. 5(a) and (b), respectively. The kinetic parameters and the corresponding correlation coefficients are given in Table 3. Based on the correlation coefficients, the biosorption of lead(II) onto Bsi20310 EPS was better described by pseudo-second-order than pseudo-first-order equation both in salt-free water and salt water. In addition, the biosorption rate constant k_2, an index of the biosorption time to reach the same uptake fraction [29], obtained from salt water (0.0052) was larger than that obtained from salt-free water (0.0040), which implied that the biosorption in salt water was faster and more favorable than that in salt-free water.

Qt versus $t^{1/2}$ plots for intraparticle diffusion model are shown in Fig. 5(c) and the parameters are given in Table 4. In these plots, two phases are observed, indicating that the sorption process was succeeded by surface sorption and intraparticle diffusion. The initial sharp portion of the plot indicated a boundary layer diffusion effect while the second linear portion was due to intraparticle diffusion [30]. The multi-linear plots implied that intraparticle diffusion was not the only rate-limiting step for the whole biosorption [7,31]. Furthermore, k_{p1} was much larger than k_{p2} in two biosorption processes, revealing that external surface biosorption was the major biosorption mechanism.

3.6. FT-IR analysis

FT-IR spectroscopy is a useful tool for understanding the mechanisms involved in lead(II) biosorption onto Bsi20310 EPS, by detecting major functional groups of Bsi20310 EPS before and after biosorption [32]. Fig. 6 shows the FT-IR transmission spectra of fresh Bsi20310 EPS, lead(II)-loaded Bsi20310 EPS in salt-free and salt water, respectively. The FT-IR spectrum of fresh Bsi20310 EPS exhibited a broad band centered at 3447 cm^{-1} due to the stretching of hydroxyl (O–H) groups on Bsi20310 EPS surface. Two weak peaks at 2929 and 2879 cm^{-1} were assigned to the stretching of methylene (CH_2) groups, and the corresponding bending peak of CH_2 groups was found at 1414 cm^{-1} [33,34]. Besides, the FT-IR spectrum exhibited the following bands: 1115 cm^{-1} (C–O–C stretching) and 1639 cm^{-1} (C=O stretching) [35,36].

After biosorption, the broad O–H stretching band and C=O stretching peak turned a little sharper and weaker. The C–O–C stretching group was observed to shift clearly from 1115 cm^{-1} to 1042 cm^{-1} in spectrum (b) and 1042 cm^{-1} in spectrum (c), respectively. These indicated that the groups on Bsi20310 EPS surface, such as hydroxyl (–OH), carbonyl (C=O) and glycosidic (C–O–C) could be responsible for the lead(II) biosorption. Extra peaks were observed at 1741 cm^{-1} in spectrum (b) and

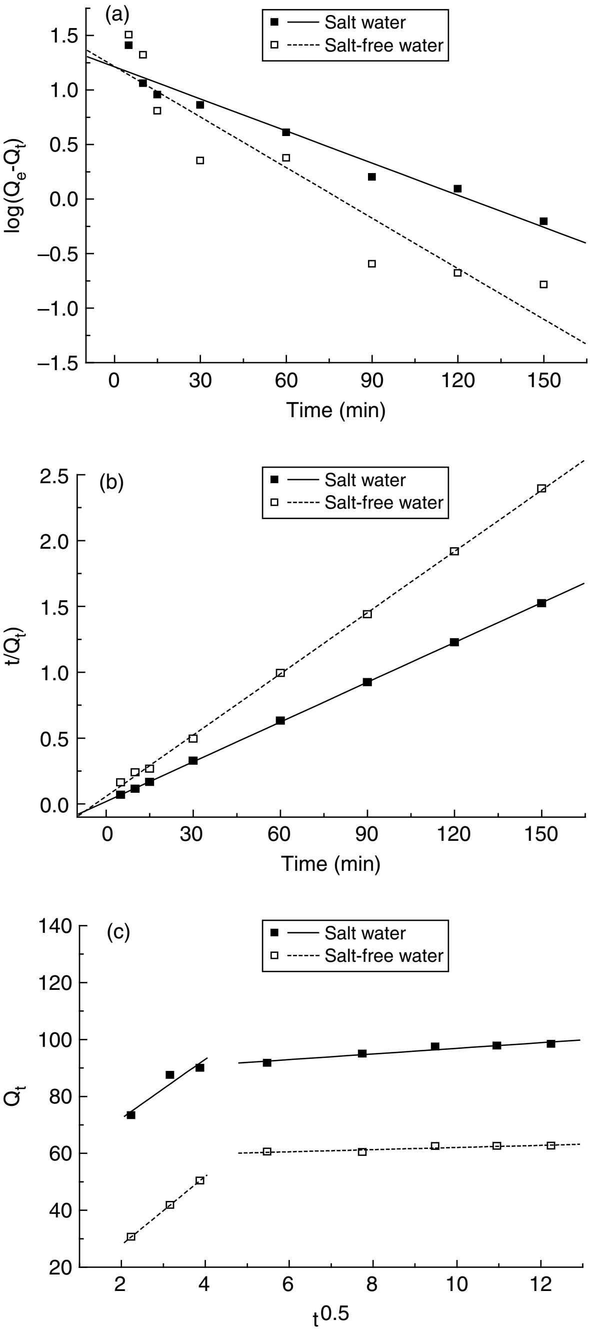

Fig. 5. Kinetic models for lead(II) biosorption onto Bsi20310 EPS (a) pseudo-first-order model; (b) pseudo-second-order model; (c) intraparticle diffusion model.

Table 3
Pseudo-first-order and pseudo-second-order kinetic parameters for lead(II) biosorption onto Bsi20310 EPS

Solution	Pseudo-first-order		Pseudo-second-order	
	k_1 (l min^{-1})	R_1^2	k_2 [g (mg min)$^{-1}$]	R_2^2
Salt-free water	0.0226	0.9524	0.0040	0.9994
Salt water	0.0356	0.8808	0.0052	0.9999

at 1743 cm^{-1} in spectrum (c), respectively. Besides, the spectra of fingerprint zone also changed after biosorption. All these changes showed that there was a metal binding process taking place on the surface of Bsi20310 EPS both in salt-free water and salt water.

The similarity between spectrum (b) and spectrum (c) indicated that the biosorption mechanism of lead(II) on EPS was similar in salt-free water and salt water. On consideration of the higher biosorption capacity of lead(II) for Bsi20310 EPS in salt water than in salt-free water, the intensity decrease in FTIR spectra of the Bsi20310 EPS for salt-free water compared to that for salt water might due to the higher retention of lead(II) by Bsi20310 EPS in salt water [37].

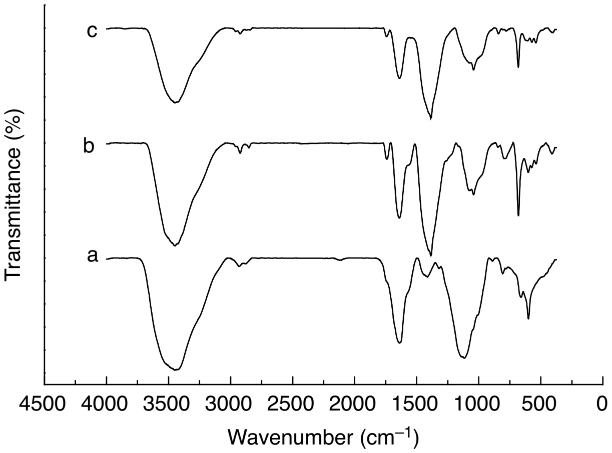

Fig. 6. FT-IR spectra (a) fresh Bsi20310 EPS; (b) lead(II)-loaded Bsi20310 EPS in salt-free water; (c) lead(II)-loaded Bsi20310 EPS in salt water.

Table 4
Intraparticle diffusion kinetic parameters for lead(II) biosorption onto Bsi20310 EPS

Solution	Initial curve			Second curve		
	k_{p1} [mg (g min$^{1/2}$)$^{-1}$]	C_1	R_{p1}^2	k_{p2} [mg (g min$^{1/2}$)$^{-1}$]	C_2	R_2^2
Salt-free water	9.33	12.96	0.8668	0.468	57.32	0.6922
Salt water	10.41	51.46	0.9063	0.992	86.98	0.9293

Acknowledgements

The authors are thankful to the supports of National Natural Science Foundation of China (50878120, 51178255), Shandong Key Scientific and Technological Projects of China (2010G0020606), Jinan Innovation Projects for Universities (201004041) and Interdisciplinary Foundation of Shandong University (2009JC017).

References

[1] M. Mohapatra, S. Khatun and S. Anand, Kinetics and thermodynamics of lead(II) adsorption on lateritic nickel ores of Indian origin, J. Chem. Eng. Data., 155 (2009) 184–190.

[2] V.S. Munagapati, V. Yarramuthi, S.K. Nadavala, S.R. Alla and K. Abburi, Biosorption of Cu(II), Cd(II) and Pb(II) by *Acacia leucocephala* bark powder: Kinetics, equilibrium and thermodynamics, J. Chem. Eng. Data., 157 (2010) 357–365.

[3] H. Chen, J. Zhao, G.L. Dai, J.Y. Wu and H. Yan, Adsorption characteristics of Pb(II) from aqueous solution onto a natural biosorbent, fallen *Cinnamomum camphora* leaves, Desalination, 262 (2010) 174–182.

[4] S.Y. Liu, J. Gao, Y.J. Yang, Y.C. Yang and Z.X. Ye, Adsorption intrinsic kinetics and isotherms of lead ions on steel slag, J. Hazard. Mater., 173 (2010) 558–562.

[5] L. Wang, J. Zhang, R. Zhao, Y. Li, C. Li and C.L. Zhang, Adsorption of Pb(II) on activated carbon prepared from *Polygonum orientale* Linn.: Kinetics, isotherms, pH, and ionic strength studies, Bioresour. Technol., 101 (2010) 5808–5814.

[6] O.S. Lawal, A.R. Sanni, I.A. Ajayi and O.O. Rabiu, Equilibrium, thermodynamic and kinetic studies for the biosorption of aqueous lead(II) ions onto the seed husk of *Calophyllum inophyllum*, J. Hazard. Mater., 177 (2010) 829–835.

[7] D. Harikishore Kumar Reddy, K. Seshaiah, A.V.R. Reddy, M. Madhava Rao and M.C. Wang, Biosorption of Pb^{2+} from aqueous solutions by *Moringa oleifera* bark: Equilibrium and kinetic studies, J. Hazard. Mater., 174 (2010) 831–838.

[8] S.H. Moon, C.S. Park, Y.J. Kim and Y. Park, Biosorption isotherms of Pb(II) and Zn(II) on Pestan, an extracellular polysaccharide, of *Pestalotiopsis* sp. KCTC 8637P, Process Biochem., 41 (2006) 312–316.

[9] B. Kiran and A. Kaushik, Chromium binding capacity of *Lyngbya putealis* exopolysaccharides, J. Biochem. Eng., 38 (2008) 47–54.

[10] H. Mokaddem, Z. Sadaoui, N. Boukhelata, N. Azouaou and Y. Kaci, Removal of Cadmium from aqueous solution by polysaccharide produced from *Paenibacillus polymyxa*, J. Hazard. Mater., 172 (2009) 1150–1155.

[11] Y. Qie, J. Wang, W.Z. Zhou, B.Y. Gao and Y.Z. Zhang, Evaluation of a deep-sea mesophilic bacteria exopolysaccharides in removal of low concentration Pb(II) from aqueous medium, Desalin. Water Treat., 28 (2011) 174–182.

[12] W.Z. Zhou, J. Wang, B.L. Shen, W.G. Hou and Y.Z. Zhang, Biosorption of copper(II) and cadmium(II) by a novel exopolysaccharide secreted from deep-sea mesophilic bacterium, Colloids Surf. B., 72 (2009) 295–302.

[13] R.P. Han, H.K. Li, Y.H. Li, J.H. Zhang, H.J. Xiao and J. Shi, Biosorption of copper and lead ions by waste beer yeast, J. Hazard. Mater., 137 (2006) 1569–1576.

[14] G. Dönmez and N. Kocherber, Bioaccumulation of hexavalent chromium by enriched microbial cultures obtained from molasses and NaCl containing media, Process Biochem., 40 (2005) 2493–2498.

[15] A.E. Ofomaja, E.I. Unuabonah and N.A. Oladoja, Competitive modeling for the biosorptive removal of copper and lead ions from aqueous solution by Mansonia wood sawdust, Bioresour. Technol., 101 (2010) 3844–3852.

[16] G. Dönmez and Z. Aksu, Removal of chromium (VI) from saline wastewaters by *Dunaliella* species, Process Biochem., 38 (2002), 751–762.

[17] D.N. Thomas1 and G.S. Dieckmann, Antarctic sea-ice—a habitat for extremophiles, Science, 295 (2002) 641–644.

[18] C.A. Mancuso Nichols, J. Guezennec and J.P. Bowman, Bacterial exopolysaccharides from extreme marine environments with special consideration of the southern ocean, sea-ice, and deep-sea hydrothermal vents: A review, Mar. Biotechnol., 7 (2005) 253–271.

[19] W.Z. Zhou, B.L. Shen, F.P. Meng and Y.Z. Zhang., Coagulation enhancement of exopolysaccharide secreted by an Antarctica sea-ice bacterium on dye wastewater, Sep. Purif. Technol., 76 (2010) 215–221.

[20] J. Bollmann, J.O. Herrle, M.Y. Cortés and S.R. Fielding, The effect of sea water salinity on the morphology of *Emiliania huxleyi* in plankton and sediment samples, Earth Planet. Sci. Lett., 284 (2009) 320–328.

[21] A. Mishra and B. Jha, Isolation and characterization of extracellular polymeric substances from micro-algae *Dunaliella salina* under salt stress, Bioresour. Technol., 100 (2009) 3382–3386.

[22] I. Vyrides and D.C. Stuckey, Adaptation of anaerobic biomass to saline conditions: Role of compatible solutes and extracellular polysaccharides, Enzyme Microb. Technol., 44 (2009) 46–51.

[23] B. Southichak, K. Nakano, M. Nomura, N. Chiba and O. Nishimura, A novel biosorbent for the removal of heavy metals from aqueous solution, Water Res., 40 (2006) 2295–2302.

[24] C. Jeon and K.H. Park, Adsorption and desorption characteristics of mercury(II) ions using aminated chitosan bead, Water Res., 39 (2005) 3938–3944.

[25] G.R. Carlos, R.T. Victor and G.G. Bruno, Cadmium and zinc removal from aqueous solutions by *Bacillus jeotgali*: pH, salinity and temperature effects, Bioresour. Technol., 99 (2008) 3864–3870.

[26] D. Harikishore Kumar Reddy, Y. Harinath, K. Seshaiah and A.V.R. Reddy, Biosorption of Pb(II) from aqueous solutions using chemically modified *Moringa oleifera* tree leaves, Chem. Eng. J., 162 (2010) 626–634.

[27] J.C.P. Vaghetti, E.C. Lima, B. Royer, B.M. da Cunha, N.F. Cardoso, J.L. Brasil and S.L.P. Dias, Pecan nutshell as biosorbent to remove Cu(II), Mn(II) and Pb(II) from aqueous solutions, J. Hazard. Mater., 162 (2009) 270–280.

[28] M. Iqbal, A. Saeed and S.I. Zafar, FTIR spectrophotometry, kinetics and adsorption isotherms modeling, ion exchange, and EDX analysis for understanding the mechanism of Cd^{2+} and Pb^{2+} removal by mango peel waste, J. Hazard. Mater., 164 (2009) 161–171.

[29] Y. Li, Q.Y. Yue and B.Y. Gao, Adsorption kinetics and desorption of Cu(II) and Zn(II) from aqueous solution onto humic acid, J. Hazard. Mater., 178 (2010) 455–461.

[30] L. Wang, J. Zhang, R. Zhao, Y. Li, C. Li and C. Zhang, Adsorption of Pb(II) on activated carbon prepared from *Polygonum orientale* Linn.: Kinetics, isotherms, pH, and ionic strength studies, Bioresour. Technol., 101 (2010) 5808–5814.

[31] B.H. Hameed, Equilibrium and kinetics studies of 2,4,6-trichlorophenol adsorption onto activated clay, Colloid Surf. A., 307 (2007) 45–52.

[32] S. Pradhan, S. Singh and L.C. Rai, Characterization of various functional groups present in the capsule of *Microcystis* and study of their role in biosorption of Fe, Ni and Cr, Bioresour. Technol., 98 (2007) 595–601.

[33] A. Kamari and W.S. Wan Ngah, Isotherm, kinetic and thermodynamic studies of lead and copper uptake by H_2SO_4 modified chitosan, Colloids Surf. B., 73 (2009) 257–266.

[34] C.G. Kumar, H.S. Joo, J.W. Choi, Y.M. Koo and C.S. Chang, Purification and characterization of an extracellular polysaccharide from haloalkalophilic *Bacillus* sp. I-450, Enzyme Microb. Technol., 34 (2004) 673–681.

[35] Y.P. Wang, Z. Ahmed, W. Feng, C. Li and S.Y. Song, Physicochemical properties of exopolysaccharide produced by *Lactobacillus kefiranofaciens* ZW3 isolated from Tibet kefir, Int. J. Biol. Macromol., 43 (2008) 283–288.

[36] H. Yazıcı, M. Kılıç and M. Solak, Biosorption of copper(II) by *Marrubium globosum* subsp. *globosum* leaves powder: Effect of chemical pretreatment, J. Hazard. Mater., 151 (2008) 669–675.

[37] G. Blazque, M. Calero, F. Hernaiz, G. Tenorio and M.A. Martin-Lara, Equilibrium biosorption of lead(II) from aqueous solutions by solid waste from olive-oil production, J. Chem. Eng., 160 (2010) 615–622.